INSTITUTE OF PHYSICS PUBLISHING NONLINEARITY

Nonlinearity **18** (2005) 125–138 doi:10.1088/0951-7715/18/1/007

Stability of n-dimensional patterns in a generalized Turing system: implications for biological pattern formation

Mark Alber[1,4], **Tilmann Glimm**[2], **H G E Hentschel**[2], **Bogdan Kazmierczak**[1] **and Stuart A Newman**[3]

[1] Department of Mathematics, 255 Hurley Building, University of Notre Dame, Notre Dame, IN 46556-4618, USA
[2] Department of Physics, Emory University, Atlanta, GA 30322-2430, USA
[3] Department of Cell Biology & Anatomy, Basic Science Building, New York Medical College, Valhalla, NY 10595, USA

E-mail: malber@nd.edu, tglimm@emory.edu, phshgeh@physics.emory.edu, bkazmie1@nd.edu and newman@nymc.edu

Received 27 April 2004, in final form 29 July 2004
Published 1 October 2004
Online at stacks.iop.org/Non/18/125

Recommended by J A Glazier

Abstract
The stability of Turing patterns in an n-dimensional cube $(0, \pi)^n$ is studied, where $n \geqslant 2$. It is shown by using a generalization of a classical result of Ermentrout concerning spots and stripes in two dimensions that under appropriate assumptions only sheet-like or nodule-like structures can be stable in an n-dimensional cube. Other patterns can also be stable in regions comprising products of lower-dimensional cubes and intervals of appropriate length. Stability results are applied to a new model of skeletal pattern formation in the vertebrate limb.

PACS numbers: 87.10.+e, 87.18.La, 87.18.Hf

Mathematics Subject Classification: 92C15, 92C37, 37N25, 46N60

1. Introduction

Reaction–diffusion systems, in which self-organizing instabilities arising from the coupling of chemical reactions with diffusion lead to nonuniform patterns of chemical concentration, have received much attention from mathematicians and physicists since Turing first analysed them half a century ago [1] (see, amongst others, [2] and [3] for a review). While theoretical

[4] Author to whom any correspondence should be addressed.

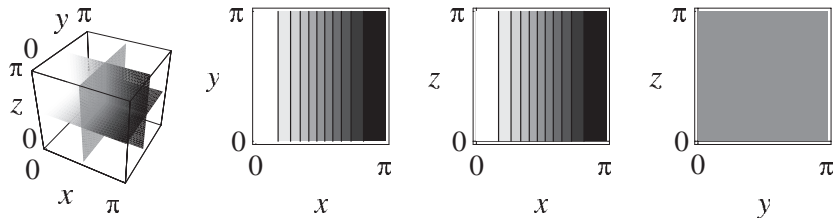

Figure 1. Density plots of $u(x, y, z) = \cos x$ in the cube $[0, \pi]^3$ with cross-sections at $z = \pi/2$, $y = \pi/2$ and $x = \pi/2$, respectively. We call this pattern a (three-dimensional) $\frac{1}{2}$-*sheet*.

applications of reaction–diffusion models to various problems in biological pattern formation followed upon Turing's paper [4–7], serious consideration of this class of mechanisms by biologists only began once a reaction–diffusion mechanism was shown unambiguously to underlie pattern formation in an experimental (chemical) system [8, 9].

In [10], a new reaction–diffusion model was introduced to explain the process of precartilage condensation in the embryonic chick limb. The proposed mechanism models the first stage in the development of the limb skeletal pattern. This 'bare bones' model consists of a system of three equations that describe the spatiotemporal distribution of two morphogens and the density of precartilage ('mesenchymal') cells that respond to these heterogeneous morphogen distributions via haptotaxis (see [10] for a review of the biology). These equations are capable of producing patterns via a Turing bifurcation, a mechanism by which some components of an initial distribution corresponding to unstable modes of a system linearized around a homogeneous steady state undergo exponential growth, whereas all other modes decay exponentially. It is thus that patterns emerge from initially small perturbations of a spatially homogeneous base state.

In nonlinear systems, the exponential growth is eventually slowed down by higher order terms. Typically, the system then reaches a steady state. It is therefore of interest to study the stability of these patterns under small perturbations, as all steady states corresponding to the patterns observed in experiments must be stable.

In [11], it is shown that patterns obtained close to a Turing-type instability of a reaction–diffusion system defined in a two-dimensional square can be of just two types, stripes or spots. General criteria are also given for the stability of reaction–diffusion patterns in a two-dimensional square (subject to no-flux boundary conditions) near a spatially homogeneous steady state. This result is obtained using the Lyapunov–Schmidt reduction method and group theoretic considerations (see [12] and [13]). For $n = 3$ a similar result was obtained in [16]. The approach of [16] is different from the one used in [11]. It is based on purely group theoretic considerations and it does not take into account the specific form of the system of equations.

In biological applications one mostly deals with three-dimensional structures. The structures we are interested in can be described by their cross-sections perpendicular to the limb's long axis. We distinguish between sheet-like, bar-like and nodule-like structures (see figures 1–3). Sheet-like structures have two stripe-like cross-sections and one unpatterned cross-section. Bar-like structures have two stripe-like cross-sections and one spot-like cross-section, whereas nodule-like patterns have spot-like cross-sections in all dimensions.

In modelling skeletal pattern formation during vertebrate embryogenesis, the bones of the vertebrate limb can be identified with three-dimensional bars or nodules. For example, the avian forelimb skeletal elements can be roughly decomposed (starting at the proximal shoulder and continuing to the distal tip of the wing) as consisting of one skeletal bar (the 'humerus') followed by two skeletal bars (the 'radius' and 'ulna') followed by the nodule-like carpal and tarsal structures of the wrist and ankle and finally a number of segmented bar-like

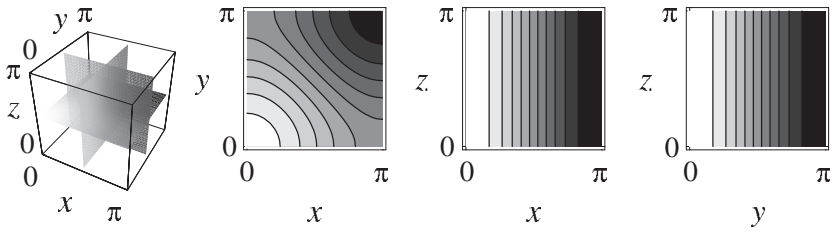

Figure 2. Density plots of $u(x, y, z) = \cos x + \cos y$ in the cube $[0, \pi]^3$ with cross-sections at $z = \pi/2$, $y = \pi/2$ and $x = \pi/2$, respectively. We call this pattern a (three-dimensional) $\frac{1}{2}$-*bar*.

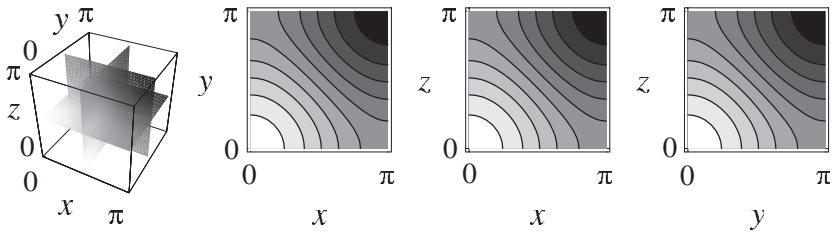

Figure 3. Density plots of $u(x, y, z) = \cos x + \cos y + \cos z$ in the cube $[0, \pi]^3$ with cross-sections at $z = \pi/2$, $y = \pi/2$ and $x = \pi/2$, respectively. We call this pattern a (three-dimensional) $\frac{1}{2}$-*nodule*.

structures (the 'digits'). A complete analysis of the conditions under which each of these three-dimensional patterns is stable is therefore of great importance.

This paper focuses on obtaining explicit conditions for stability of patterns obtained via a Turing bifurcation phenomenon in three or more dimensions, and their application to a problem of precartilage condensation in the avian limb within the context of the model proposed in [10]. This model in its simplest form couples a Turing-like pattern forming a reaction–diffusion system to a mechanism for cellular differentiation (see section 5). The differentiated cells can release an insoluble substrate adhesive molecule ('fibronectin') into the extracellular matrix that results in cell migration via haptotaxis up the fibronectin gradients.

We derive these stability conditions by extending the method from [11], and develop stability criteria for patterns in n-dimensional cubes, where $n \geqslant 2$, for a general system of reaction–diffusion equations. This method takes into account the specific form of the equations. The scalar parameters appearing in the stability conditions obtained are explicitly determined by the coefficients of the system. We are thus able to control the stability of patterns by altering these coefficients. More specifically, they can be expressed using second and third order terms in the Taylor expansion around the steady state. Therefore, we can ensure stability of patterns by adding appropriate terms of order 2 or 3. The effects of second order terms are difficult to study analytically as they result in complicated expressions. On the other hand, addition of third order terms does not significantly complicate the analysis.

We show that only n-dimensional nodules or n-dimensional sheets can be stable in an n-dimensional cube although not at the same time. We also show that other patterns such as bars can be stable in any region that is a Cartesian product of an $n-1$-dimensional cube and an interval of sufficiently small length. This is of particular significance in modelling the vertebrate limb, where the main skeletal structures are bars (cf remark 2.2).

Finally, we apply our results to the three-dimensional model of vertebrate skeletal development [10]. Since our method is system-specific, we are able to investigate the stability of patterns by changing the rate at which the cells produce fibronectin, the extracellular matrix

molecule that provides an adhesive substratum for the cells. We show that under certain conditions there exists a threshold for fibronectin production that separates stable sheets from stable nodules. This is a very encouraging result for the validity of the model since a similar phenomenon has been observed experimentally in cultures of cells derived from embryonic chicken wings and legs. That is, levels of fibronectin produced by cells derived in chicken wing buds are lower than in leg buds. Wing condensations in culture are broad and flat (i.e. sheet-like) whereas leg condensations are compact and spherical (i.e. nodule-like) [18].

The theoretical results described in this paper have been used in numerical implementation of two- and three-dimensional multiscale models of vertebrate limb development in [19, 20].

This paper is organized as follows. In section 2 we describe our approach to analysing Turing bifurcations in an n-dimensional cube. We also indicate how to treat the more general case of a parallelepiped. Section 3 contains stability results. In section 4 we investigate the effect of third order terms. This is followed in section 5 by an application of our results to the model of the vertebrate limb. Finally, we conclude with a discussion of the implications of our results for the patterning observed in the developing limb.

2. General method

As mentioned in section 1 our method follows the general strategy of [11]. It is based on representing the solution u as well as the bifurcation parameter $\tilde{\lambda}$ in the form of a power series in terms of a small parameter ε. Substitution into the considered system, comparison of terms for the same powers of ε and application of the Fredholm alternative procedure result in a set of relations from which stability conditions are derived.

2.1. Turing bifurcation

Consider a system of nonlinear equations of reaction–diffusion type on an n-dimensional domain $\mathbb{R}^n$ ($n \geqslant 2$),

$$-D\nabla^2 \boldsymbol{U} = \mathcal{F}(\boldsymbol{U}, \tilde{\lambda}). \tag{2.1}$$

Here $\boldsymbol{U} = (U_1, \ldots, U_m) : \Omega \to \mathbb{R}^m$ ($m \geqslant 2$), and $\mathcal{F} = (F_1, \ldots, F_m)$, $m \geqslant 2$, is a family of sufficiently smooth vector-valued mappings that depend on a bifurcation parameter $\tilde{\lambda} \in \mathbb{R}^1$. D is a constant $m \times m$ matrix whose m eigenvalues are all positive.

Assumption 1. *There exists a constant steady state $\boldsymbol{U}_0$ of system (2.1). To be more precise, $\mathcal{F}(\boldsymbol{U}_0, \tilde{\lambda}) = 0$ for all $\tilde{\lambda}$. Moreover, this steady state is stable with respect to spatially homogeneous pertubations, that is, all the eigenvalues of the linearization matrix $\partial\mathcal{F}/\partial u(\boldsymbol{U}_0, 0)$ have negative real parts.*

Let us denote

$$A = \frac{\partial \mathcal{F}}{\partial \boldsymbol{U}}(\boldsymbol{U}_0, 0), \qquad u = \boldsymbol{U} - \boldsymbol{U}_0.$$

Then in the vicinity of $\boldsymbol{U}_0$, system (2.1) can be written as

$$(-A - D\nabla^2)u = \mathcal{Q}(u, u) + \mathcal{C}(u, u, u) + \tilde{\lambda}\mathcal{B}u + \text{h.o.t.}, \tag{2.2}$$

where $\mathcal{Q}(u, u)$ and $\mathcal{C}(u, u, u)$ are second and third order terms in the Taylor series of $\mathcal{F}$ around $\boldsymbol{U} = \boldsymbol{U}_0$. The operator $\mathcal{B}$ can have a very general form. In this paper, we assume that

$$\mathcal{B} = B_1 + B_2\nabla^2,$$

where B_1 and B_2 are constant $m \times m$ matrices.

In the case of $n = 2$ a general form of system (2.2) was analysed in [11]. In this paper, we consider equation (2.2) in the n-dimensional cube

$$\Omega = (0, \pi)^n, \qquad n \geqslant 2.$$

Assume that $\boldsymbol{U}$ satisfies *no-flux* boundary conditions [5], i.e.

$$\frac{\partial \boldsymbol{U}}{\partial n}(x_1, \ldots, x_n) = 0 \qquad \text{for } (x_1, \ldots, x_n) \in \partial\Omega. \tag{2.3}$$

Here n is an outward normal vector at the boundary $\partial\Omega$. (Biologically, equation (2.3) means that there is no boundary leakage. This assumption is often plausible in mathematical models.) Notice that u satisfies the same boundary conditions

$$\frac{\partial u}{\partial n}(x_1, \ldots, x_n) = 0 \qquad \text{for } (x_1, \ldots, x_n) \in \partial\Omega. \tag{2.4}$$

Assumption 2. *The trivial solution $u = 0$ to problems (2.2) and (2.4) is stable for $\tilde{\lambda} < 0$ and unstable for $\tilde{\lambda} > 0$. In other words, the following operator*

$$u \mapsto D\nabla^2 u + Au + \tilde{\lambda}\mathcal{B}u, \tag{2.5}$$

where u satisfies (2.4), has only negative eigenvalues for $\tilde{\lambda} < 0$, at least one positive eigenvalue for $\tilde{\lambda} > 0$ and zero eigenvalue for $\tilde{\lambda} = 0$.

In the case considered below, the zero eigenvalue is not simple and its geometric multiplicity is equal to n (see lemma 1).

As a consequence of assumption 2, the operator in (2.5) has a nontrivial kernel for $\tilde{\lambda} = 0$. Therefore, there is a nontrivial function u_0 such that $Au_0 + D\nabla^2 u_0 = 0$.

The family of functions $\prod_i \cos(k_i x_i)$, where k_i are nonnegative integers, forms a basis of the space of functions in Ω that satisfy zero-flux boundary conditions. (This follows from the Stone–Weierstrass theorem; see, e.g., [17].) Thus, we can write u_0 in the form

$$u_0 = \sum_{\boldsymbol{k}} \boldsymbol{a}^{\boldsymbol{k}} \prod_{i=1,\ldots,n} \cos(k_i x_i) = 0,$$

where $\boldsymbol{k} = (k_1, \ldots, k_n)$. Consequently, the following relation must be satisfied:

$$\sum_{\boldsymbol{k}} (-\boldsymbol{k}^2 D + A)\boldsymbol{a}^{\boldsymbol{k}} \psi_{\boldsymbol{k}}(x) = 0,$$

where $\psi_{\boldsymbol{k}}(x) = \prod_{i=1,\ldots,n} \cos(k_i x_i)$. Now, as the functions $\psi_{\boldsymbol{k}}$ are linearly independent in Ω, then for every $\boldsymbol{k}$ we have that

$$(-\boldsymbol{k}^2 D + A)\boldsymbol{a}^{\boldsymbol{k}} = 0. \tag{2.6}$$

A and D are $m \times m$ matrices and, therefore, in general, this equation can have nonunique linearly independent eigenvalue pairs $(\boldsymbol{k}^2, \boldsymbol{a}^{\boldsymbol{k}})$. However, in what follows we make an assumption that in (2.6) $\boldsymbol{a}^{\boldsymbol{k}} \neq 0$ only when $\boldsymbol{k}^2 = 1$. We discuss below to what extent this assumption constitutes a restriction on the general case.

[5] Note that the normal component of the flux $\boldsymbol{J}_i$ of the term u_i $(i = 1, \ldots, m)$ at the point $(x_1, \ldots, x_n) \in \delta\Omega$ has the form

$$\boldsymbol{J}_i \cdot n = \left[-\sum_{j=1,\ldots,m} D_{ij} \nabla U_j \right] \cdot n = -\sum_{j=1,\ldots,m} D_{ij} \frac{\partial U_j}{\partial n}(x_1, \ldots, x_n).$$

Hence, by assuming boundary conditions $\boldsymbol{J}_i \cdot n = 0$, $i = 1, \ldots, m$, and matrix D being invertible, we obtain expression (2.3). We call these expressions no-flux boundary conditions.

Assumption 3. *The matrix* $(A-D)$ *has a unique eigenvalue equal to* 0 *with the corresponding eigenvector* $\boldsymbol{e}$. *All other* $(m-1)$ *eigenvalues have negative real parts. Moreover, for any* $\boldsymbol{k}^2 \neq 1$, *the matrix* $A - \boldsymbol{k}^2 D$ *has only negative eigenvalues.*

The following lemma follows from this last assumption.

Lemma 1. *Functions* $u_{0\ell} = \boldsymbol{e}\cos x_\ell$, $\ell = 1, \ldots, n$, *span space of solutions to the equation* $Au_0 + D\nabla^2 u_0 = 0$ *in the cube* $\Omega = (0,\pi)^n$. *In other words, operator (2.5) has an* n*-dimensional kernel for* $\tilde{\lambda} = 0$.

Proof. If $\boldsymbol{k}^2 = 1$, then due to (2.6) $\boldsymbol{a}^{\boldsymbol{k}}$ must be a multiple of $\boldsymbol{e}$, so that the general solution to the equation $Au_0 + D\nabla^2 u_0 = 0$ has the form $\sum_{\ell=1,\ldots,n} a_\ell \boldsymbol{e}\cos(x_\ell)$. This concludes the proof of the lemma.

We are interested in the solutions $(u, \tilde{\lambda})$ to the steady state equation (2.2) bifurcating from the constant steady state at $\tilde{\lambda} = 0$. Suppose that this bifurcating solution is parametrized by ε; that is, we consider a solution $(u_\varepsilon, \lambda_\varepsilon)$ to the equation

$$(A + D\nabla^2)u_\varepsilon \mathcal{Q}(u_\varepsilon, u_\varepsilon) + \mathcal{C}(u_\varepsilon, u_\varepsilon, u) + \tilde{\lambda}_\varepsilon \mathcal{B}u_\varepsilon = 0. \tag{2.7}$$

We represent $(u_\varepsilon, \lambda_\varepsilon)$ in the form of power series in terms of ε:

$$u_\varepsilon = \varepsilon u_0 + \varepsilon^2 u_1 + \cdots, \tag{2.8}$$

$$\tilde{\lambda}_\varepsilon = \varepsilon^2 \lambda + \cdots. \tag{2.9}$$

After comparing first order terms in ε in equation (2.7) and using lemma 1 we obtain that

$$u_0(x_1, \ldots, x_n) = (s_1 \cos x_1 + \cdots + s_n \cos x_n)\boldsymbol{e}.$$

So up to the first order terms, the patterns can be generated by using linear combinations of the elementary patterns $\cos x_i$.

We call a special pattern corresponding to the case when $s_1 = \cdots = s_n$ an n-dimensional nodule. (It looks like a 'blob' in one corner of the cube.) Another special pattern corresponds to the case when $s_i \neq 0$ for some $i = 1, \ldots, n$, but $s_\ell = 0$ for $\ell \neq i$. We call such a pattern an n-dimensional $\frac{1}{2}$-sheet pattern.

Before we present our result on the stability of these patterns, which generalizes the result of Ermentrout [11] in two dimensions, we discuss the case of a more general domain.

2.2. Case of a general domain

In this section, we make three suggestions on how our assumptions can be extended leading to analysis of more general patterns as well as more general domains.

Aspect ratios. Our assumptions may be generalized to incorporate also many-sheet patterns. One can achieve this simply by considering the system in a different domain. For example, if we are interested in M_i-half-sheet elementary patterns in x_i, where $M_1, \ldots M_n$ are nonnegative integers, then it suffices to consider the system in the parallelepiped

$$\tilde{\Omega} = \prod_{i=1}^{n} (0, M_i\pi). \tag{2.10}$$

In this general case, a basis for the family of functions that satisfy no-flux boundary conditions is given by the functions $\prod_i \cos(m_i x_i / M_i)$, where $m_1, \ldots, m_n$ are nonnegative integers. If the dimension of the kernel is to be equal to n as in lemma 1, we must impose an additional

condition in accordance with the condition $\sum k_i^2 = 1$. Namely, we allow only sets of positive integers $M_1, \ldots, M_n$ that satisfy the following condition:

If $m_1, \ldots, m_n$ are nonnegative integers such that

$$\left(\frac{m_1}{M_1}\right)^2 + \left(\frac{m_2}{M_2}\right)^2 + \cdots + \left(\frac{m_n}{M_n}\right)^2 = 1, \tag{2.11}$$

then there is an index i^* such that $m_{i^*} = M_{i^*}$ and $m_i = 0$ for $i \neq i^*$.

For example, in dimensions $n = 2$ and $n = 3$, this condition is satisfied for the cubes $\tilde{\Omega} = (0, 2\pi)^n$. (This is the case when $M_1 = M_2 = 2$ and $M_3 = 2$.) Such a domain, for $n = 2$, was considered in [11]. However, note that for dimension $n \geqslant 4$, the n-dimensional cube $(0, 2\pi)^n$ does *not* satisfy this condition.

Dimensional reduction. Let $\tilde{\Omega}$ be an n-dimensional parallelepiped as before with $\{M_i\}_{j=1}^n$ satisfying condition (2.11). Suppose now that α is an irrational number and consider equation (2.2) in the $(n + 1)$-dimensional parallelepiped $\tilde{\Omega}' = \tilde{\Omega} \times (0, \alpha\pi)$. A basis of the functions satisfying no-flux conditions on $\tilde{\Omega}'$ now consists of

$$\cos\left(\frac{m_{n+1}x_{n+1}}{\alpha}\right)\prod_{i=1}^{n}\cos\left(\frac{m_i x_i}{M_i}\right).$$

Lemma 1 still holds in $\tilde{\Omega}'$ and stable patterns are still formed by linear combinations of $\cos(x_i)$, $i = 1, \ldots, n$. This remains true for any positive number $\alpha < 1$ (not just irrational ones).

This also indicates that analysis of patterns on a square Ω can be extended to a parallelepiped with base Ω and small height h. For instance, a single spot in the centre of the square Ω corresponds to a bar of height h in the parallelepiped. We note that in the developing skeleton of the vertebrate limb, a three-dimensional case in which the main elements are bars, the height in the dorsoventral (back to front; e.g. back of the hand to palm) dimension is always small relative to the other two dimensions.

New scales. Finally, note that rescaling the domain Ω is equivalent to rescaling function $\mathcal{F}(u)$ in (2.2). For example, consider system (2.2) in the cube $(0, \pi)^n$. Introducing the new scaling $x' = \sqrt{g}x$ is equivalent to modification of the expression

$$\left(-\frac{1}{g}A - D\nabla_{x'}^2\right)u = \frac{1}{g}(\mathcal{Q}(u, u) + \mathcal{C}(u, u, u)) + \tilde{\lambda}\mathcal{B}'u + \text{h.o.t.}$$

considered in the cube $\Omega' = (0, \sqrt{g}\pi)^n$ where $\nabla_{x'}^2$ denotes the Laplacian with respect to x'. Here we incorporated the factor $1/g$ in front of $\mathcal{B}'u$ into $\tilde{\lambda}$.

3. Stability of patterns

In this section, we prove stability of the bifurcating solutions (2.8). Stability is studied by comparing two parameters a and b associated with the system. We follow Ermentrout [11] in introducing the following definitions.

Let $\boldsymbol{f}$ be an eigenvector satisfying

$$\boldsymbol{f}(A - D) = 0, \qquad \boldsymbol{f} \cdot \boldsymbol{e} = 1.$$

Also let

$$L_0 = -A, \qquad L_2 = -A + 2D, \qquad L_4 = -A + 4D.$$

These matrices are invertible according to the uniqueness of k^2 satisfying assumption 2. Define the following constants

$$\begin{aligned} &\alpha_0 = \boldsymbol{f}\mathcal{Q}(\boldsymbol{e}, L_0^{-1}\mathcal{Q}(\boldsymbol{e},\boldsymbol{e})), \qquad &&\alpha_4 = \boldsymbol{f}\mathcal{Q}(\boldsymbol{e}, L_4^{-1}\mathcal{Q}(\boldsymbol{e},\boldsymbol{e})), \\ &\alpha_2 = 4\boldsymbol{f}\mathcal{Q}(\boldsymbol{e}, L_2^{-1}\mathcal{Q}(\boldsymbol{e},\boldsymbol{e})), \qquad &&\beta = \boldsymbol{f}\mathcal{C}(\boldsymbol{e},\boldsymbol{e},\boldsymbol{e}), \qquad \mu = \boldsymbol{f}\cdot B\boldsymbol{e}. \end{aligned} \tag{3.12}$$

Here $\mathcal{Q}$ and $\mathcal{C}$ are the quadratic and cubic terms as in (2.2), and B is a matrix determined as follows: $\mathcal{B}(\boldsymbol{e}\cos x_\ell) = B\boldsymbol{e}\cos x_\ell$. Finally, we set

$$a = \alpha_0 + \frac{1}{2}\alpha_4 + \frac{3}{4}\beta, \qquad b = \alpha_0 + \frac{1}{2}\alpha_2 + \frac{3}{2}\beta. \tag{3.13}$$

Now we can introduce the following generalization of a theorem by Ermentrout [11].

Theorem 1. *Consider the bifurcating solution*

$$u_\varepsilon(x) = \varepsilon(s_1\cos x_1 + \cdots + s_n\cos x_n)\boldsymbol{e} + \varepsilon^2 u_1 + \cdots$$

to equation (2.7) as in (2.8).

1. *There is an integer p $(1 \leqslant p \leqslant n)$ such that*

$$|s_1| = \cdots = |s_p| \neq 0, \qquad s_{p+1} = \cdots = s_n = 0$$

   (after a permutation of the indices of $x_1, \ldots, x_n$, if necessary).
2. *The stability of u_ε is determined as follows:*
   (a) $p = 1$: *u_ε is stable iff $b < a < 0$,*
   (b) $p = n$: *u_ε is stable iff $a < \min\{b, -(n-1)b\}$,*
   (c) $1 < p < n$: *u_ε is* always *unstable.*

Note that for $p = 1$ the density plot of u_ε is an n-dimensional $\frac{1}{2}$-sheet. For $p = n$ and $s_1 = \cdots = s_n$, the contour plot is a single n-dimensional nodule (see figures 1 and 3 for the case $n = 3$). The theorem asserts that only n-dimensional sheets or nodules can be stable, but never for the same set of parameters. *No* other pattern can be stable.

Proof. We first derive the reduced bifurcation equations. Consider the equation

$$(A + D\nabla^2)u_\varepsilon + \mathcal{Q}(u_\varepsilon, u_\varepsilon) + \mathcal{C}(u_\varepsilon, u_\varepsilon, u_\varepsilon) + \tilde{\lambda}_\varepsilon \mathcal{B}u_\varepsilon = 0. \tag{3.14}$$

First order terms in ε yield that $(A + D\nabla^2)u_0 = 0$, from which it follows that

$$u_0 = (s_1\cos x_1 + \cdots + s_n\cos x_n)\boldsymbol{e}.$$

Comparison of second order terms in ε results in the following equation:

$$(A + D\nabla^2)u_1 = -\mathcal{Q}(u_0, u_0) = \frac{1}{2}\mathcal{Q}(\boldsymbol{e},\boldsymbol{e})\left(\sum_i s_i^2(1 + \cos(2x_i)) + \sum_{i\neq j} s_i s_j \cos x_i \cos x_j\right),$$

which yields that

$$u_1 = \sum_{i\neq j} s_i s_j \cos x_i \cos x_j L_2^{-1}\mathcal{Q}(\boldsymbol{e},\boldsymbol{e}) + \frac{1}{2}\sum_i s_i^2 L_0^{-1}\mathcal{Q}(\boldsymbol{e},\boldsymbol{e}) + \frac{1}{2}\sum_i s_i^2\cos(2x_i)L_4^{-1}\mathcal{Q}(\boldsymbol{e},\boldsymbol{e}).$$

Finally, third order terms in ε in (3.14) yield

$$(A + D\nabla^2)u_2 + 2\mathcal{Q}(u_0, u_1) + \mathcal{C}(u_0, u_0, u_0) + \lambda\mathcal{B}u_0 = 0.$$

Multiply this equation by $\cos x_\ell \boldsymbol{f}^T$ on the left for $\ell = 1, \ldots, n$ and integrate over $\Omega = [0, \pi]^n$. This results in the following system of n reduced equations:

$$0 = s_\ell\left(\mu\lambda + a s_\ell^2 + b\sum_{i\neq\ell} s_i^2\right), \qquad \ell = 1, \ldots, n. \tag{3.15}$$

Certain $(n-p)$ of the s_ℓ are zero, where $1 \leqslant p \leqslant n$. Without loss of generality we assume that $s_{p+1} = \cdots = s_n = 0$. The first p coefficients s_ℓ satisfy

$$\begin{pmatrix} a & b & b & \cdots & b \\ b & a & \ddots & \ddots & \vdots \\ b & \ddots & \ddots & \ddots & b \\ \vdots & \ddots & \ddots & a & b \\ b & \cdots & b & b & a \end{pmatrix} \begin{pmatrix} s_1^2 \\ \vdots \\ s_p^2 \end{pmatrix} = -\mu\lambda \begin{pmatrix} 1 \\ \vdots \\ 1 \end{pmatrix}.$$

It follows that $s_1^2 = \cdots = s_p^2 \equiv s^2$ and s^2 satisfies $[a+(p-1)b]s^2 = -\mu\lambda$. The Jacobian of the right-hand side of the reduced bifurcation system (3.15) evaluated at $s_1, \ldots, s_n$ with $s_1^2 = \cdots s_p^2 = s^2$, $s_{p+1} = \cdots = s_n = 0$, is equivalent to the matrix

$$Jac = \begin{pmatrix} A_p & 0 \\ 0 & B_p \end{pmatrix}$$

with the submatrices

$$A_p = 2(a-b)s^2\mathbb{I}_p + 2bs^2\mathbf{1}_p, \qquad B_p = (\mu\lambda + bps^2)\mathbb{I}_{n-p}.$$

Here $\mathbb{I}_p$ denotes the $p \times p$ identity matrix and $\mathbf{1}_p$ denotes the $p \times p$ matrix with unit entries. Note that $\mathbf{1}_p$ has eigenvalues p and 0 with multiplicities 1 and $(p-1)$, respectively.

The eigenvalues $\lambda_1, \ldots, \lambda_n$ of *Jac* are as follows:

$$\begin{aligned} &\lambda_1 = 2(a-b)s^2 + 2pbs^2 = -2\mu\lambda, \\ &\lambda_2 = \cdots = \lambda_p = 2(a-b)s^2, \\ &\lambda_{p+1} = \cdots = \lambda_n = \lambda\mu + bps^2 = -s^2(a-b). \end{aligned}$$

According to a theorem by Sattinger ([13], theorem 4.3, p 82), solution u_ε is stable if and only if all the eigenvalues λ_i, $i = 1, \ldots, n$, are negative. For $p = 1$ this condition is equivalent to $a < 0$ and $a > b$. For $p = n$ we get $a < -(n-1)b$ and $a < b$. For $1 < p < n$, one gets the contradicting conditions $a < b$ and $a > b$. This completes the proof. □

4. Influence of third order terms on the stability

In what follows we study how a given system can be altered in order to produce stable nodules or sheets. Note that the expressions for the parameters a and b from (3.13), which are used to determine stability, depend on both second and third order terms. The fact that the stability of patterns is affected not only by second order terms but equally by third order terms may seem somewhat surprising at first. An analysis of the proof of theorem 1 shows how third order terms come into play. That is, the power series of the bifurcation parameter $\tilde{\lambda}$ starts with ε^2 (see equation (2.9)). Hence, one needs to compare terms up to *third* order in ε in equation (3.14) to arrive at the reduced equations (3.15) involving λ.

We ensure stability of patterns by adding appropriate terms of order 2 or 3. The effects of second order terms are hard to study analytically because they result in complicated expressions. On the other hand, addition of third order terms does not result in complications in the analysis. Also changing the third order terms affects the solution very little if it is close to the bifurcating constant state.

We present our results in the form of the following two theorems. Theorem 2 says that *any* system can be modified by adding third order terms in such a way that it would have stable

n-dimensional sheets. On the other hand, theorem 3 states that only those systems that satisfy condition $2a - b < 0$ can be modified to have stable nodules.

Theorem 2. *Consider system (2.2) with Turing instability for $k^2 = 1$ around a spatially homogeneous steady state* $\mathbf{0}$*. Then there exist numbers κ_i, $i = 1, 2, \ldots, n$ such that for the system*

$$(-A - D\nabla^2)u = \mathcal{Q}(u, u) + \mathcal{C}(u, u, u) + Ku^3 + \tilde{\lambda}\mathcal{B}u + \text{h.o.t.}, \tag{4.16}$$

where $K = \{K_{ij}\} = \{\kappa_i \delta_{ij}\}$, $u^3 = (u_1^3, \ldots, u_n^3)^T$, n-dimensional sheets are stable solutions obtained via the Turing bifurcation.

Proof. Note first that addition of the third order term $K(u, u, u)$ to the right-hand side of equation (4.16) results in β changing to $\beta + \Delta\beta$, where

$$\Delta\beta = \sum_{i=1}^{n} f_i \kappa_i (e_i)^3,$$

and a changing to $a_{\Delta\beta} = a + \frac{3}{4}\Delta\beta$ and b changing to $b_{\Delta\beta} = b + \frac{3}{2}\Delta\beta$. Recall that $\boldsymbol{f} \cdot \boldsymbol{e} = 1$. Therefore, at least for one m we have $f_m e_m \neq 0$. Thus, we may choose the numbers κ_i in such a way that the number $\Delta\beta$ attains any given value.

Now, by choosing a negative $\Delta\beta$ with large enough modulus, we can guarantee that the following double inequality holds:

$$b_{\Delta\beta} < a_{\Delta\beta} < 0.$$

This is the set of sufficient conditions for stability of n-dimensional sheets. □

For nodules, the situation is slightly more complicated. In fact, not every system (2.2) can be modified by adding only third order terms to have stable nodules. That is, such a system needs to satisfy the following necessary and sufficient condition.

Theorem 3. *Consider system (2.2) with Turing instability for $k^2 = 1$ around a spatially homogeneous steady state* $\mathbf{0}$*. Then the following statements are equivalent:*

(i) $2a - b < 0$*;*

(ii) *there exists a third order term $K(u, u, u) = \sum_{ij\ell} \boldsymbol{\kappa}_{ij\ell} u_i u_j u_\ell$ such that for the system*

$$(-A - D\nabla^2)u = \mathcal{Q}(u, u) + \mathcal{C}(u, u, u) + K(u, u, u) + \tilde{\lambda}\mathcal{B}u + \text{h.o.t.}, \tag{4.17}$$

nodules are stable solutions obtained via Turing bifurcation.

Proof. We use the same notation as in the previous proof. After adding the third order term, β changes to $\beta + \Delta\beta$, while a changes to $a_{\Delta\beta} = a + \frac{3}{4}\Delta\beta$ and b changes to $b_{\Delta\beta} = b + \frac{3}{2}\Delta\beta$.

Suppose first that condition (ii) is satisfied, that is, after adding the above third order terms, we have

$$a_{\Delta\beta} < \min\{b_{\Delta\beta}, -(n-1)b_{\Delta\beta}\}.$$

It follows that $a_{\Delta\beta} \leqslant 0$ and, therefore, $2a_{\Delta\beta} \leqslant a_{\Delta\beta} < b_{\Delta\beta}$. This implies that condition (i) is satisfied if $2a - b = 2a_{\Delta\beta} - b_{\Delta\beta} < 0$.

Now suppose that condition (i) is satisfied. As shown in the proof of theorem 2, we may choose the third order term Ku^3 such that $\Delta\beta = -\frac{2}{3}b$. Then $b_{\Delta\beta} = 0$ and

$$a_{\Delta\beta} = a - \tfrac{1}{2}b < 0 = \min\{b_{\Delta\beta}, -(n-1)\, b_{\Delta\beta}\}.$$

This is a sufficient condition for the stability of nodules. Therefore, condition (ii) is satisfied. □

5. Application to a model of skeletal pattern formation

In this section, we use the general approach described in the previous sections for studying stability of patterns in a model of skeletal pattern formation proposed in [10].

5.1. Description of the model

We consider the following system of reaction–diffusion equations:

$$\frac{\partial}{\partial t}\boldsymbol{U} = g\mathcal{F}(\boldsymbol{U}) + (D(\lambda_2) + dH)\nabla^2\boldsymbol{U}, \tag{5.18}$$

where $\boldsymbol{U} = (u, v, R)$ and

$$\mathcal{F}(\boldsymbol{U}) = \begin{pmatrix} (J_a(u)\beta(u) + J_a^1\alpha(u))R - uv \\ J_i(u)\beta(u)R - uv \\ rR(R_0 - R) \end{pmatrix}, \qquad H = \begin{pmatrix} 0 & 0 & 0 \\ 0 & 1 & 0 \\ 0 & 0 & 0 \end{pmatrix},$$

$$D(\lambda_2) = \begin{pmatrix} 1 & 0 & 0 \\ 0 & 0 & 0 \\ -\lambda_2\dfrac{\partial\gamma}{\partial u}R^2 & 0 & d_{\text{cell}} - \lambda_2\gamma(u)R \end{pmatrix}.$$

We consider these equations on a rectangular domain with no-flux boundary conditions. The variables $u(x, t)$ and $v(x, t)$ are the concentrations of certain morphogens (the diffusible protein factor TGF-β, which induces fibronectin production, and an inhibitor of TGF-β). There are three different types of mobile mesenchymal cells in this model, namely type R_1, type R_2 and type $R_{2'}$ cells. The concentrations of these different types of cells are given as fractions of the overall cell density $R(x, t)$ as $R_1(x, t) = \alpha(u)R(x, t)$, $R_2(x, t) = \beta(u)R(x, t)$ and $R_2'(x, t) = \gamma(u)R(x, t)$, where $\alpha + \beta + \gamma = 1$. (A fourth cell type, R_3, corresponding to the nonmobile cartilage cell that differentiates from the $R_{2'}$ cells, is considered in the full model [10] but does not enter into the reaction–diffusion system.) Note that the proportions α, β and γ depend on the TGF-β concentration u. The R1 cells produce TGF-β and the inhibitor at the rates $J_a(u)$ and $J_i(u)$, respectively, whereas R2 cells produce TGF-β at the low constant rate J_a^1. R2′ cells secrete the extracellular matrix molecule fibronectin, which is known to initiate adhesion-mediated mesenchymal condensation. In the equations above, the parameter λ_2 is directly related to the rate at which R2′ cells produce fibronectin.

The diffusion coefficient of TGF-β is scaled to 1, while the diffusion coefficients of the inhibitor and the cells are denoted by d and d_{cell}, respectively. Note that there is an effective diffusion coefficient for the cells $d_{\text{effective}} = d_{\text{cell}} - \lambda_2\gamma(u)R$ in the above equations as diffusion of cells is slowed down in the presence of fibronectin. The parameter g is directly related to the scale of the domain [6].

One is mainly interested in spatial patterns in the cell density R arising in these equations through a Turing-type mechanism as described in section 2. Sites of high cell concentration are interpreted as the onset of mesenchymal precartilage condensation.

It is shown in [10] that for certain parameter ranges system (5.18) can give rise to patterns via a Turing-type mechanism. Here we are interested in the stability of these patterns. Indeed,

[6] In biological systems, signals may be propagated by a combination of direct cell–cell communication and active cell response in a fashion that is mechanistically different from, but formally analogous to, free diffusion [21]. In such cases, the stability problem would be very different from that described here. Simulations using realistic biological parameters have indicated, however, that true diffusion (specifically of TGF-β class morphogens like that considered here) is a plausible component of developmental pattern-forming mechanisms [21].

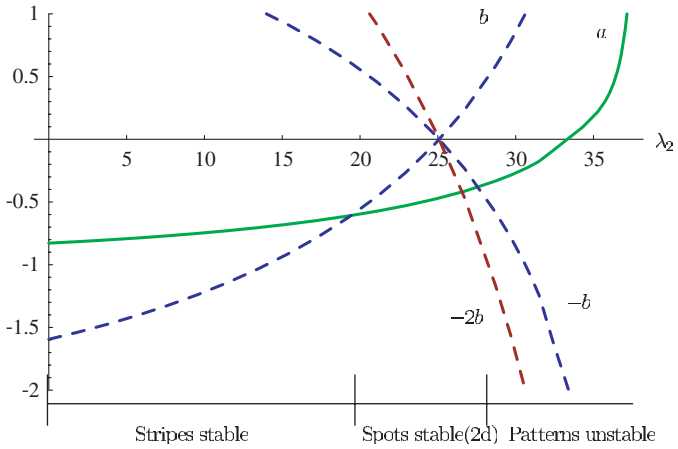

Figure 4. Plot of $a(\lambda_2)$ and $b(\lambda_2)$ with intervals of stability.
(This figure is in colour only in the electronic version)

it seems reasonable that any patterns one can observe in experiments must be stable with respect to small perturbations, although there could of course be other mechanisms not accounted for in the above 'bare-bones' model that stabilize the emerging patterns.

5.2. Examples of stable patterns

We carried out a study of the influence of the fibronectin production rate λ_2 on the stability of patterns (see figure 4). Let us first indicate how system (5.18) fits in the general set-up of the previous sections.

Fix all parameters except d and λ_2. Let $\boldsymbol{U}_0 = (u_0, v_0, R_0)$ denote the constant equilibrium of (5.18) meaning that $\mathcal{F}(\boldsymbol{U}_0) = 0$. As before, denote by $A = (\partial\mathcal{F}/\partial\boldsymbol{U})(\boldsymbol{U}_0)$ the linearization of the kinetic terms at the equilibrium.

Now, for each λ_2 there exists a critical value $d_{\text{crit}} = d_{\text{crit}}(\lambda_2)$ of d and a number k_0^2 such that there is an onset of a Turing bifurcation at the mode k_0. That is, the matrix $gA - k_0^2(D - d_{\text{crit}}H)$ has a one-dimensional kernel and all other eigenvalues are negative. Also, for any $k^2 \neq k_0^2$ all eigenvalues of $gA - k^2(D - d_{\text{crit}}H)$ are negative. The parameter g can be used for rescaling k_0^2 to 1. Then the steady state equation for system (5.18) in the vicinity of $d = d_{\text{crit}}$ is given by

$$0 = g\,\mathcal{F}(\boldsymbol{U}) + (D(\lambda_2) + d_{\text{crit}}H)\nabla^2\boldsymbol{U} + (d - d_{\text{crit}})H\nabla^2\boldsymbol{U}. \tag{5.19}$$

This equation has the form of the general bifurcation equation (2.2). Our bifurcation parameter is $\tilde{\lambda} = d - d_{\text{crit}}$.

In a way similar to section 3, we now compute parameters a and b (which in this case are functions of λ_2) and determine the stability of patterns using the criteria of theorem 1. Figure 4 presents graphs of a and b as functions of λ_2 for the following parameter values:

$$R_0 = 2.0, \qquad \beta(u) = \frac{0.745\,147u}{u + 1.922\,48}, \qquad \gamma(u) = \frac{0.031\,3087u}{u + 1.922\,48},$$

$$J_a(u) = \frac{260.0u}{u + 5.7}, \qquad J_i(u) = \frac{286.26u}{u + 5.5}, \qquad J_0 = 0.78, \qquad r = 5.0, \qquad d_{\text{cell}} = 0.65.$$

Now by using figure 4 and theorem 1 we can identify the following intervals.

Two-dimensional case (square):

$0 \leqslant \lambda_2 < 19.4$: stripes are stable ($b < a < 0$),
$19.4 < \lambda_2 < 27.6$: spots are stable ($a < \min(b, -b)$),
$\lambda_2 > 27.6$: no pattern is stable.

Three-dimensional case (cube):

$0 \leqslant \lambda_2 < 19.4$: sheets are stable ($b < a < 0$),
$19.4 < \lambda_2 < 26.6$: nodules are stable ($a < \min(b, -2b)$),
$\lambda_2 > 26.6$: no pattern is stable.

6. Discussion

In this paper, we have investigated patterns generated by means of a Turing bifurcation in n-dimensional cubes. We showed that such patterns were linear combinations of $\frac{1}{2}$-sheet patterns. We also derived a stability criterion (theorem 1) and showed that only $\frac{1}{2}$-sheets and n-dimensional nodules could be stable. We proved that for any given system, sheets could be made stable by adding third order terms. This is not the case for nodules; instead we obtained a necessary and sufficient condition for determining the cases when nodules could be made stable by adding third order terms.

Finally, we have applied the stability criteria to a model of skeletal pattern formation in the chicken limb [10]. The conditions under which different sheet-like and nodule-like patterns are stable are crucial to our understanding of the different generic skeletal elements that are observed in the avian limb. In the context of avian limb development this is clearly seen in the initial stability of the bar-like humerus, radius and ulna, followed by the nodule-like carpals and tarsals and finally the bar-like digits (though there appears to be a new segmentation transition being observed here).

Theoretical results described in this paper have been used in the numerical implementation of two-dimensional and three-dimensional multiscale models of vertebrate limb development in [19, 20].

It is interesting to see in our stability analysis of the biological equations that the parameter λ_2 (which is directly related to the rate of fibronectin production of the cells) determines the stability of different patterns. This is encouraging since, as mentioned in the introduction, that the level of fibronectin appears to play the predicted role in the shape of precartilage condensations *in vitro* [18], a phenomenon that also emerges in a biologically-motivated cellular automata model of precartilage condensation *in vitro* [22].

In fact, in biological systems the stability criterion may turn out to be even more complex than considered in this paper. In particular, the domain in which the pattern appears has an asymmetrical paddle-like shape, and is also subject to anisotropic growth along various axes (in the case of an avian limb these would correspond to the proximodistal—shoulder to limb tip—anteroposterior—thumb to little finger—and dorsoventral—back surface to palm—axes [23]). The stability problem may thus include a convective component, which may also influence the stability of the biological pattern.

While our analysis was carried out for Cartesian domains, the methods used in this paper can be applied also to domains Ω of more general shapes. In this case, however, instead of cosine functions one would have to work with the eigenfunctions of the operator (2.5) (with $\tilde{\lambda} = 0$). By applying the general procedure described above, one could arrive at a stability theorem resembling theorem 1, but the calculations would be algebraically more difficult due to the more complicated properties of the eigenfunctions corresponding to the zero

eigenvalue [12–15]. Of course, the resulting patterns may differ from the patterns obtained for a rectangular domain.

In addition, boundary conditions, other than the no-flux conditions that we considered in this paper, will certainly have an effect on the patterns and their stability.

Acknowledgments

This work was supported by NSF Grant No IBN-0083653. We acknowledge support from the Center for Applied Mathematics and the Interdisciplinary centre for the Study of Biocomplexity at the University of Notre Dame.

References

[1] Turing A 1952 The chemical basis of morphogenesis *Phil. Trans. R. Soc.* B **237** 37–72
[2] Cross M C and Hohenberg P 1993 Pattern formation outside of equilibrium *Rev. Mod. Phys.* **65** 851–1112
[3] Crampin E J and Maini P K 2001 Reaction–diffusion models for biological pattern formation *Methods Appl. Anal.* **8** 415–28
[4] Keller E F and Segel L A 1970 Initiation of slime mold aggregation viewed as an instability *J. Theor. Biol.* **26** 399–415
[5] Gierer A and Meinhardt H 1972 A theory of biological pattern formation *Kybernetik* **12** 30–39
[6] Kauffman S A, Shymko R M and Trabert K 1978 Control of sequential compartment formation in Drosophila *Science* **199** 259–70
[7] Newman S A and Frisch H L 1979 Dynamics of skeletal pattern formation in developing chick limb *Science* **205** 662–8
[8] Castets V, Dulos E, Boissonade J and DeKepper P 1990 Experimental evidence of a sustained standing Turing-type nonequilibrium chemical pattern *Phys. Rev. Lett.* **64** 2953–6
[9] Ouyang Q and Swinney H 1991 Transition from a uniform state to hexagonal and striped Turing patterns *Nature* **352** 610–12
[10] Hentschel H G E, Glimm T, Newman S A and Glazier J A 2004 Dynamical mechanisms for skeletal pattern formation in the vertebrate limb *Proc. R. Soc.* B **271** 1713–22
[11] Ermentrout B 1991 Stripes or spots? Nonlinear effects in bifurcation of reaction–diffusion equations on the square *Proc. R. Soc.* A **434** 413–17
[12] Sattinger D 1973 *Topics in Stability and Bifurcation Theory* (*Lecture Notes in Mathematics* vol 309) (Berlin: Springer)
[13] Sattinger D 1979 *Group Theoretic Methods in Bifurcation Theory* (*Lecture Notes in Mathematics* vol 762) (Berlin: Springer)
[14] Ioss G and Joseph D D 1980 *Elementary Stability and Bifurcation Theory* (New York: Springer)
[15] Grinrod P 1991 *Patterns and Waves: The Theory and Applications of Reaction–Diffusion Equations* (Oxford: Clarendon)
[16] Callahan T K and Knobloch E 1997 Symmetry breaking bifurcations on cubic lattices *Nonlinearity* **10** 1179–216
[17] Folland G 1999 *Real Analysis* (New York: Wiley)
[18] Downie S A and Newman S A 1994 Morphogenetic differences between fore and hind limb precartilage mesenchyme: relation to mechanisms of skeletal pattern formation *Devel. Biol.* **162** 195–208
[19] Izaguirre J A *et al* 2004 CompuCell, a multi-model framework for simulation of morphogenesis *Bioinformatics* **20** 1129–37
[20] Chaturvedi R, Huang C, Kazmierczak B, Schneider T, Izaguirre J A, Newman S A, Glazier J A and Alber M 2004 *On Multiscale Approaches to 3-Dimensional Modeling of Morphogenesis* submitted
[21] Lander A D, Nie Q and Wan F Y 2002 Do morphogen gradients arise by diffusion? *Devel. Cell* **2** 785–96
[22] Kiskowski M A, Alber M S, Thomas G L, Glazier J A, Bronstein N B, Pu J and Newman S A 2004 Interplay between activator–inhibitor coupling and cell-matrix adhesion in a cellular automation model for chondrogenic patterning *Devel. Biol.* **271** 372–87
[23] Newman S A 1988 Lineage and pattern in the developing vertebrate limb *Trends Genet.* **4** 329–32